ChemComm

COMMUNICATION

Supporting Information for

In-situ Electrochemically Activated Stainless Steel-Derived NiFe Hydroxide for Highly Efficient and Stable Oxygen Evolution Reaction

Ziran Tang[1], Shangye Tang[1], Xingyan Zhang[2,3], Yufeng Liu[2,3], Yanan Zhou,[b,c] Haijun Zhou[b,c] and Shengxia Yang[2,3,*]

[a] Pegasus California School, Qingdao 266071, PR China.

[b] Institute of Carbon Neutrality, College of Chemical and Biological Engineering, Shandong University of Science and Technology, Qingdao 266590, PR China.

[c] Qingdao Perovskite Photovoltaic and Application Engineering Research Center, Shandong University of Science and Technology, Qingdao 266590, PR China;

Experimental

1.1 Chemicals

304A stainless steel mesh (The elemental makeup of the stainless steel is detailed in Table S1) was obtained from Changzhou Zhongkun Screen Mesh Co., LTD. Nickel chloride hexahydrate ($NiCl_2.6H_2O$, AR), hydrochloric acid (HCl, 37%) and potassium hydroxide (KOH, 85%) were purchased from Sinopharm Chemical Reagent Co., Ltd. Deionized water with a resistivity of 18 MΩ/cm was used in all reactions. All the chemicals were used without further purification.

1.2 Synthesis of CV-SSM

Before synthesis, a 1 cm × 2 cm stainless steel mesh was cut. To remove surface oxides and oil stains, 0.5 mol/L dilute hydrochloric acid was heated to 90 °C before immersing the SSM for 10 minutes. The residual acid and salt in the SSM were then ultrasonically cleaned with absolute ethanol and deionized water, respectively. Finally, the SSM was vacuum-dried at 60 ℃ to produce a clean base material.

For the typical preparation of CV-SSM, the cleaned and dried SSM, platinum sheet electrode, and mercury-mercury oxide (Hg/HgO) were used as the working electrode, counter electrode, and reference electrode, respectively. To explore the optimal performance catalyst, cyclic voltammetry was performed by scanning the potential from 0 to 1.5 V vs. RHE in electrolytes with varying KOH concentrations (0.01, 0.0, 0.1, 0.5, and 1.0 mol/L) and a range of cycle numbers (10, 20,

25, 30, 40, and 50 cycle). The obtained samples were washed with anhydrous ethanol and deionized water, and then dried in a vacuum drying box at 60 °C.

1.3 Synthesis of FeNi-CV-SSM

For the typical preparation of FeNi-CV-SSM, in order to explore the optimal conditions for introducing nickel ion active sites, the CV-SSM obtained from the above preparation was subjected to cyclic voltammetry activation in solutions containing different Ni^{2+} concentrations (0.1, 0.5, 0.8, 1.0 and 1.5 mol/L) and different numbers of cycles (10, 20, 25, 30, 40, 50, and 80 cycle) over a potential range of 1.0 to 1.6 V vs. RHE. Subsequently, the obtained FeNi-CV-SSM was dried in a vacuum drying oven at 60 ℃. As a control, SSM was replaced with CV-SSM to prepare FeNi-SSM under the same conditions. FeNi-IF was synthesis under the same conditions as FeNi-SSM, except that the SSM was replaced with iron foam (IF) as the substrate, and a small amount of chromium was added to the nickel-ion-containing solution.

1.4 Materials Characterizations

The crystal phases of the catalysts were investigated using X-ray diffraction (XRD) on the D8ADVANCE diffractometer equipped with a Kα radiation. The chemical state of the Ni, Fe, Cr and O in catalysts were analyzed by Thermo Scientific K-alpha X-ray photoelectron spectroscopy (XPS). The catalyst morphology was examined by a ZEISS MERLIN Compact scanning electron microscope (SEM). Inductively coupled plasma mass spectrometry (ICP-MS) measurements were performed on an Agilent 7700x instrument to quantify dissolved metal ion concentrations in the electrolyte after stability tests.The high-resolution transmission electron microscopy (HRTEM) images were obtained from FEI Tecnai G2 F20 S-TWIN.

1.5 Electrochemical measurements

Electrochemical measurements were performed with a workstation in a typical three-electrode configuration, consisting of a Pt plate, a mercury-mercury oxide (Hg/HgO), and the prepared catalyst, which were used as the counter electrode, reference electrode, and working electrode, respectively. All electrochemical measurements were conducted using the Gamry 5000 electrochemical workstation in 1 M KOH solution (pH = 14) and 1 M PBS solution (pH = 7.2). The linear sweep voltammetry (LSV) polarization curves with iR compensation were obtained at the potential range from 0 to 0.7 V vs. SCE at a scan rate of 5 mV/s. Therein, all the measured potentials versus the reference electrode were converted to a

reversible hydrogen electrode (RHE) according to the equation (ERHE = ESCE + 0.059pH + 0.098 V). Impedance plots from electrochemical impedance spectroscopy (EIS) measurements were collected over a frequency range of 100 kHz to 0.1 Hz. The cyclic voltammetry (CV) data were obtained via cyclic voltammetry at scan rates of 5, 10, 15, 20, and 25 mV/s. Chronopotentiometry (CP) tests were performed at a constant current density.

Electrochemically Active Surface Area (ECSA)

The calculation of ECSA and roughness factor (RF) are based on the following equation:

$$ECSA = C_{dl}/C_s \quad (1)$$

In eq (1), C_{dl} is the measured double-layer capacitance of samples in 1 M KOH or 1 M PBS and C_s (mF) is the specific capacitance of the catalyst (C_s = 0.04 mF/cm^2 in 1 M KOH or 1 M PBS).

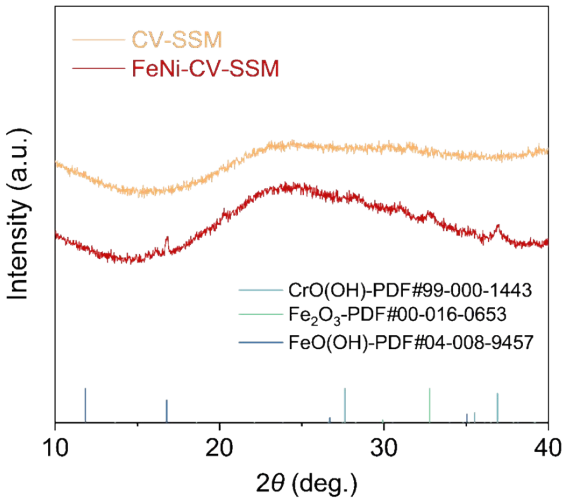

Figure S1. Magnified view of the XRD pattern of FeNi-CV-SSM in the 2θ range of 10° - 40°.

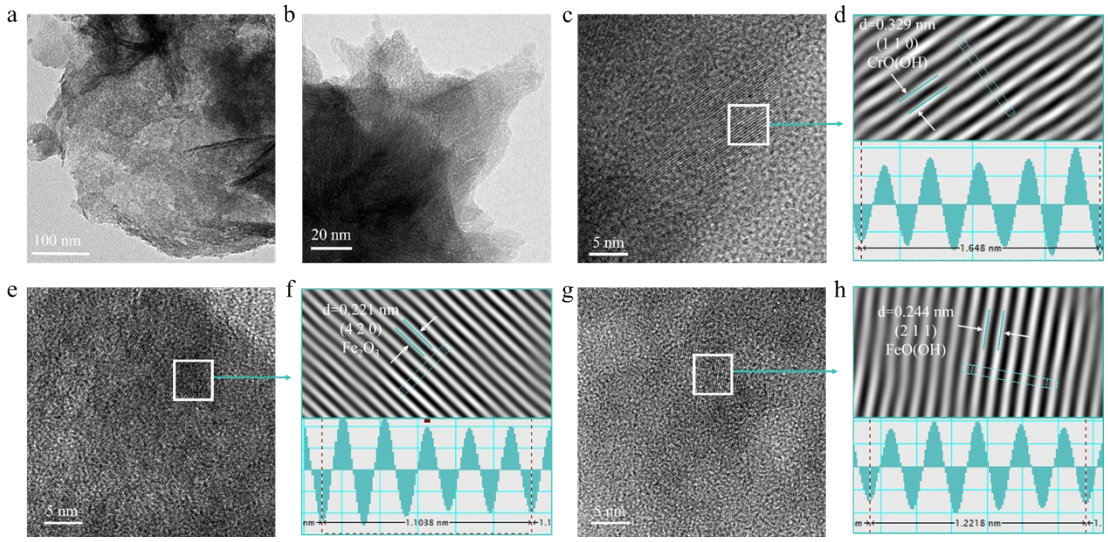

Figure S2. (a, b) TEM and HRTEM characterization of the FeNi-CV-SSM. (c-h) HRTEM images and corresponding intensity profiles showing lattice fringes of CrO(OH) (110, d = 0.329 nm), Fe_2O_3 (420, d = 0.221 nm), and FeO(OH) (211, d = 0.244 nm), respectively.

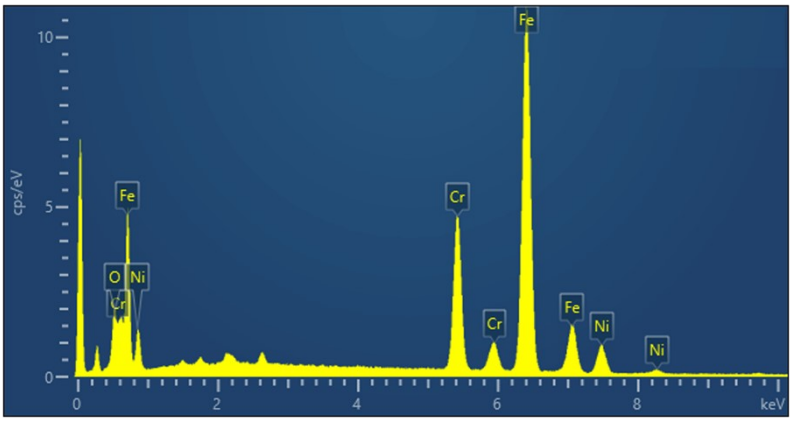

Figure S3. EDS data of the FeNi-CV-SSM.

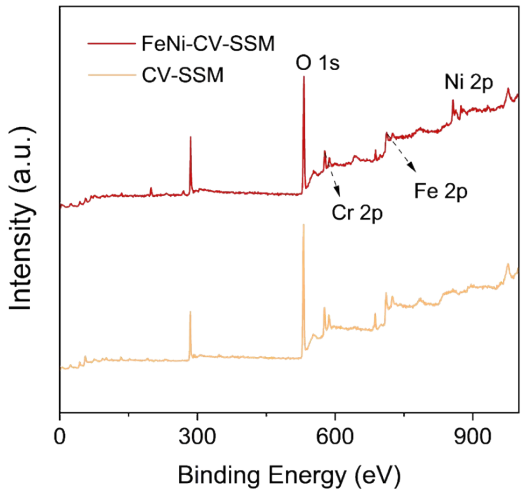

Figure S4. XPS survey spectrum of the CV-SSM and FeNi-CV-SSM samples.

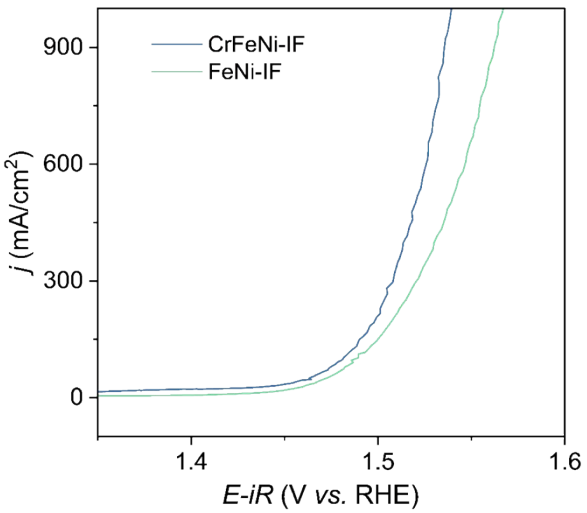

Figure S5. Linear sweep voltammetry curves of CrFeNi-IF and FeNi-IF electrodes in 1 M KOH.

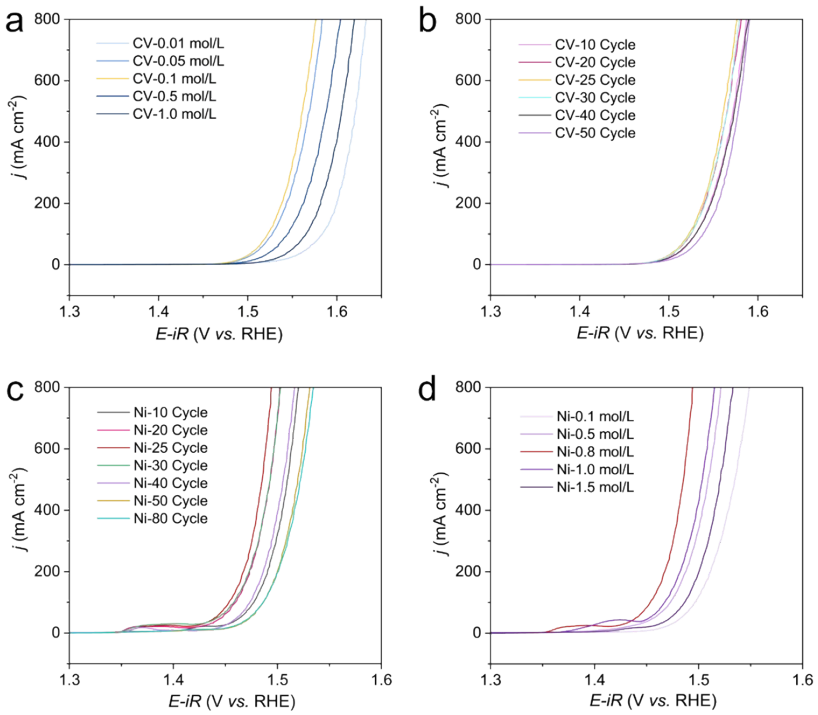

Figure S6. Polarization curves of the CV-SSM with different (a) KOH concentrations and (b) CV cycles. Polarization curves of FeNi-CV-SSM with different (c) CV-cycles and (d) Ni2+ concentrations.

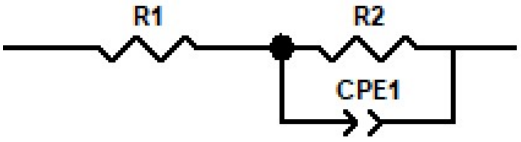

Figure S7. Schematic illustration of the equivalent circuit model used for fitting the Nyquist plots, where R1 (Rs) represents the solution resistance, R2 (Rct) is the charge transfer resistance, and CPE corresponds to the constant phase element of the double-layer capacitance.

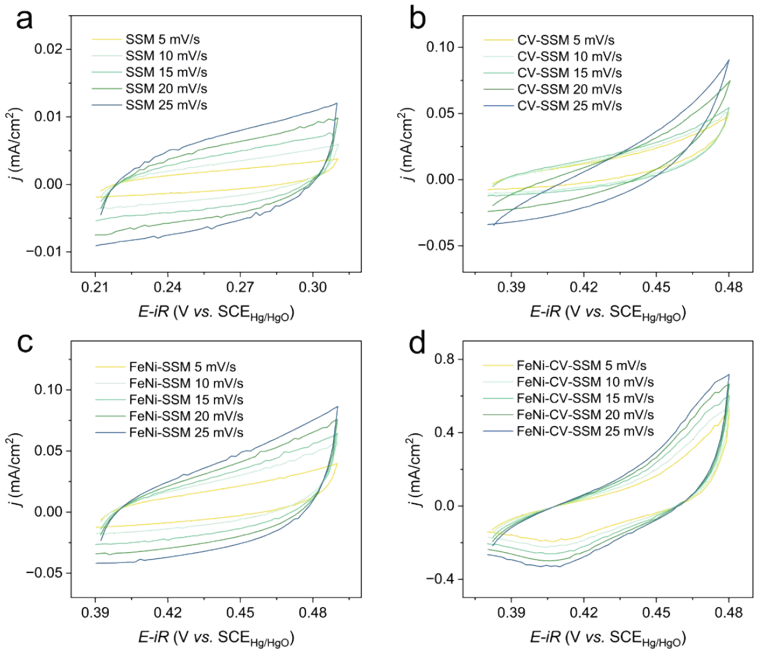

Figure S8. CV curves with iR compensation of (a) SSM, (b) CV-SSM, (c) FeNi-SSM, and (d) FeNi-CV-SSM in 1 M KOH.

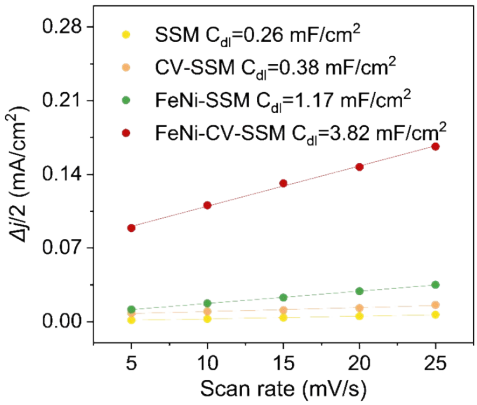

Figure S9. Cdl values without iR compensation of SSM, CV-SSM, FeNi-SSM, and FeNi-CV-SSM in 1 M KOH.

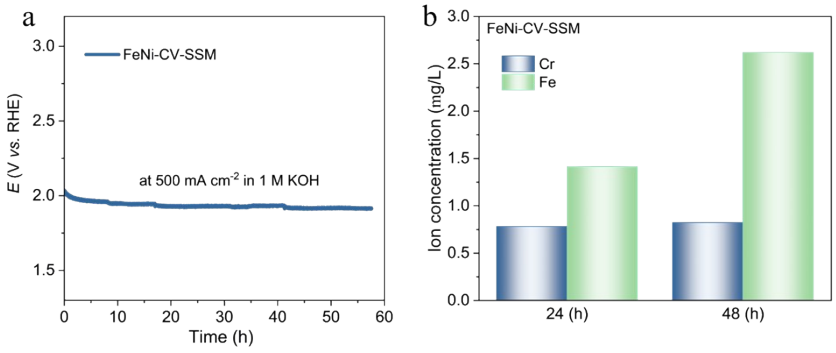

Figure S10. Long-term stability tests of FeNi-CV-SSM electrodes at 500 mA/cm^2 in 1 M KOH, and ICP-MS analysis of Fe and Cr ion concentrations in the electrolyte after 24 and 48 h of operation for FeNi-CV-SSM.

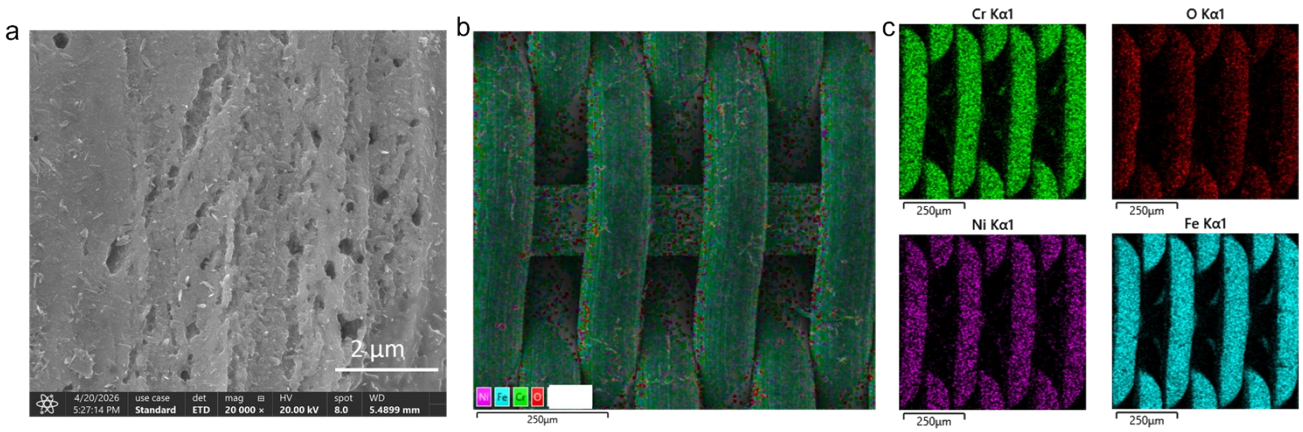

Figure S11. (a) SEM image and (b, c) corresponding elemental mapping (Cr, O, Ni, Fe) of FeNi-CV-SSM after long-term stability testing.

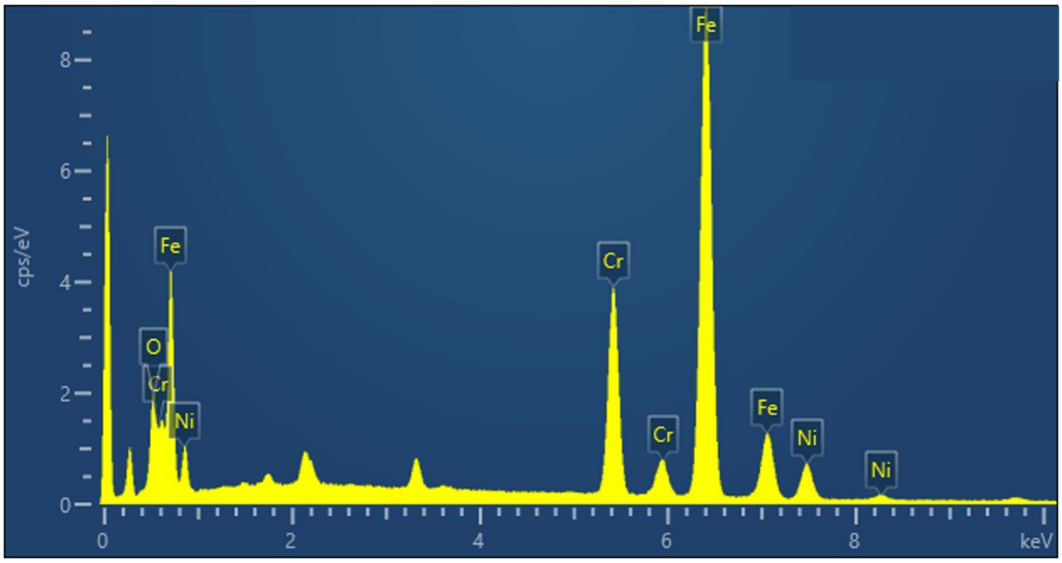

Figure S12. EDS data of FeNi-CV-SSM after 1 M KOH stability testing.

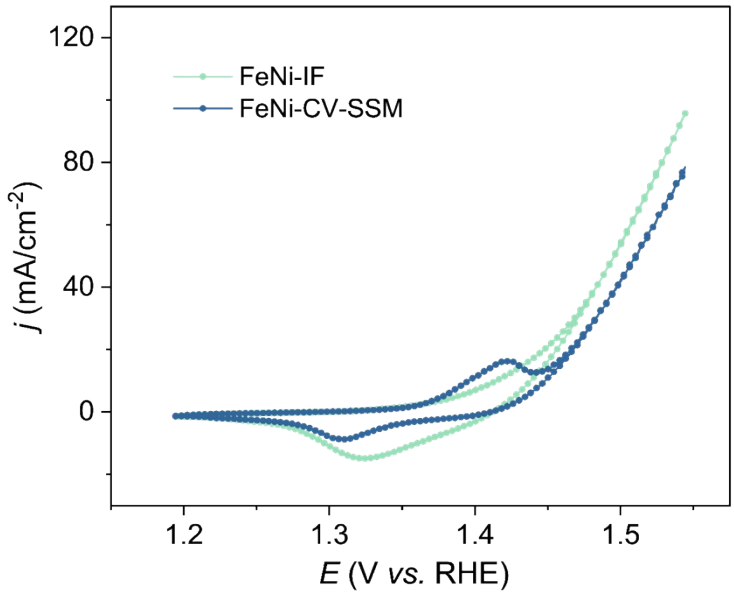

Figure S13. Cyclic voltammetry curves of FeNi-CV-SSM and FeNi-IF electrodes in 1 M KOH electrolyte.

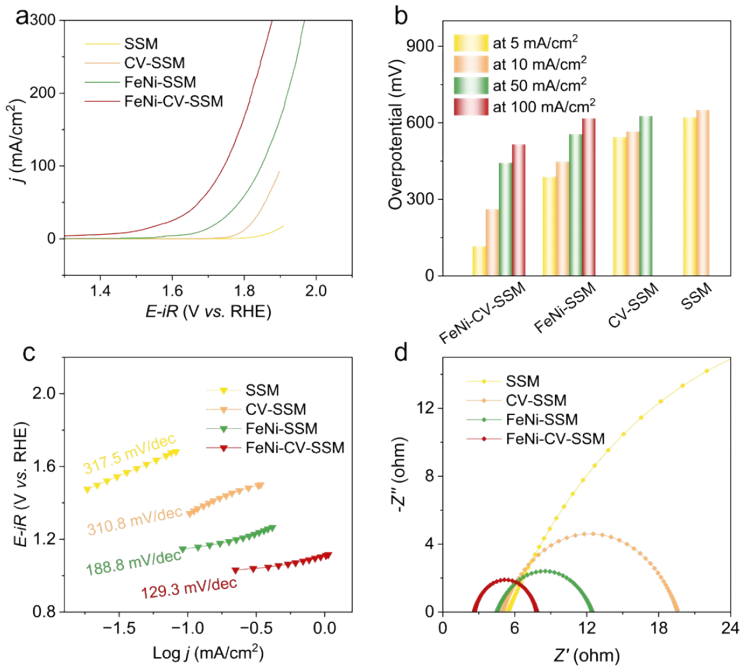

Figure S14. Comparison of (a) polarization curves and (b) overpotentials of SSM, CV-SSN, FeNi-SSM, and FeNi-CV-SSM catalysts in 1 M PBS with iR compensation. (c) Tafel and (d) Nyquist plots of different samples with iR compensation.

As shown in Figure S14a and b, FeNi-CV-SSM (η_{10} = 260 mV) has exhibited significantly enhanced oxygen evolution reaction activity in comparison with SSM (η_{10} = 650 mV), CV-SSM (η_{10} = 565 mV) and FeNi-SSM (η_{10} = 447 mV). Meanwhile, as shown in Figure S14c, FeNi-CV-SSM has displayed a lower Tafel slope (129.3 mV/dec) than SSM (371.5 mV/dec), CV-SSM (310.8 mV/dec) and FeNi-SSM (188.8 mV/dec), indicating that it has possessed fast reaction kinetics during the oxygen evolution reaction. The electron transfer kinetics have been further explored via EIS measurements (as shown in Figure S14d).

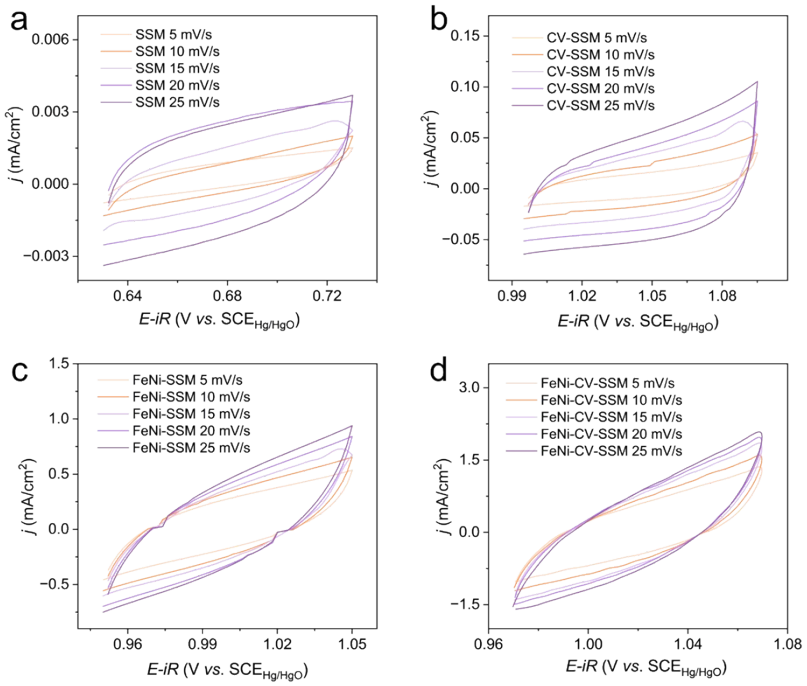

Figure S15. CV curves with iR compensation of (a) SSM, (b) CV-SSM, (c) FeNi-SSM, and (d) FeNi-CV-SSM in 1 M PBS.

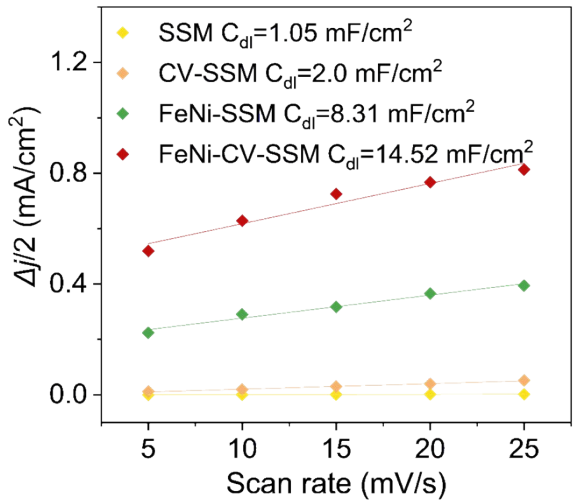

Figure S16. C_{dl} values without iR compensation in 1 M PBS.

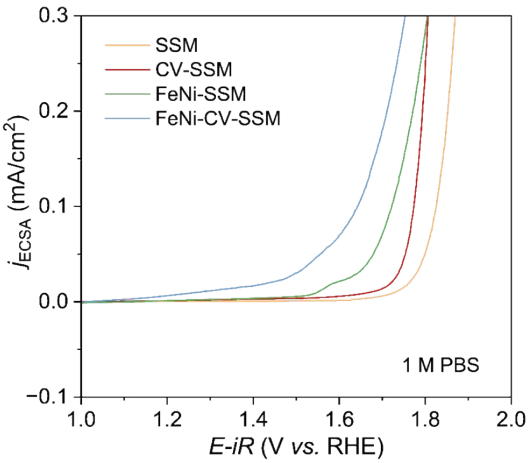

Figure 17. ECSA-normalized polarization curves of different electrodes in 1 M PBS electrolyte.

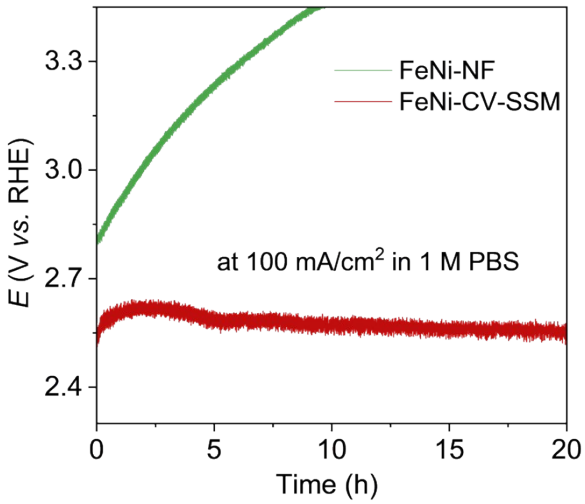

Figure S18. Chronopotentiometry curve of FeNi-NF and FeNi-CV-SSM at a current density of 100 mA/cm^2 in 1 M PBS without iR compensation.

Table S1. 304A Stainless steel mesh composition.

	Fe	Cr	Ni	Mn	S	P	C	Si
wt.%	72.369	18.10	8.05	1.00	0.009	0.04	0.052	0.38

Table S2. The EDS data of FeNi-CV-SSM.

Elements	Weight %	Atom %
O	2.89	9.22
Cr	18.51	18.38
Fe	69.98	64.71
Ni	8.62	7.58

Table S3. Fitted EIS parameters in 1 M KOH.

Sample	Rct/ohm	Rs/ohm
SSM	9.441±0.02	0.948
CV-SSM	2.837±0.02	0.721
FeNi-SSM	2.129±0.02	0.740
FeNi-CV-SSM	0.964±0.02	0.747

Table S4. The calculated ECSA values of as-prepared samples in 1 M KOH.

Sample	C_{dl} (mF)	C_s (mF/cm^2)	ECSA (cm^2)
SSM	0.26	0.04	6.5
CV-SSM	0.38	0.04	9.5
FeNi-SSM	1.17	0.04	29.25
FeNi-CV-SSM	3.82	0.04	95.5

Table S5. ICP-MS analysis results of Fe and Cr ion concentrations in the electrolyte after stability tests of FeNi-CV-SSM.

Time/h	Sampling volume/mL	Prepared solution volume/mL	Cr (mg/L)	Fe (mg/L)
24	0.500	10	0.78	1.41
48	0.500	10	0.82	2.62

Table S6. The EDS data of FeNi-CV-SSM after stability test (1 M KOH).

Elements	Weight%	Atom%
O	2.89	9.22
Cr	18.51	18.38
Fe	69.98	64.71
Ni	8.62	7.58

Table S7. Fitted EIS parameters in 1 M PBS.

Sample	Rct/ohm	Rs/ohm
SSM	57.45±0.02	5.426
CV-SSM	14.63±0.02	4.968
FeNi-SSM	7.963±0.02	4.503
FeNi-CV-SSM	5.212±0.02	2.625

Table S8. The calculated ECSA values of as-prepared samples in 1 M PBS.

Sample	Cdl (mF)	Cs (mF/cm^2)	ECSA (cm^2)
SSM	1.05	0.04	26.25
CV-SSM	2.0	0.04	50.0
FeNi-SSM	8.31	0.04	207.75
FeNi-CV-SSM	14.52	0.04	363.0

The Cdl value of FeNi-CV-SSM (14.52 mF/cm^2) has been significantly higher than those of FeNi-SSM (8.31 mF/cm^2) and CV-SSM (2.0 mF/cm^2), and its ECSA value has even reached a maximum of 363 cm^2, which has indicated that the surface area has been expanded by 7.3 times after cyclic voltammetry activation.